This article has been accepted for publication in a future issue of this journal, but has not been fully edited. Content may change prior to final publication. Citation information: DOI 10.1109/TIA.2018.2867328, IEEE Transactions on Industry Applications

Implementation of Immune Feedback Control Algorithm for Distribution Static Compensator

Manoj Badoni, Alka Singh, *Senior Member*, *IEEE* and Bhim Singh, *Fellow*, *IEEE*

***Abstract*—This paper presents an immune feedback control algorithm for a three phase Distribution Static Compensator (DSTATCOM) to mitigate several power quality problems such as harmonics, reactive power and load unbalancing at distribution level. A configuration chosen for DSTATCOM is based on a three-phase voltage source converter (VSC), which is suitably controlled as a shunt compensator for performing these functions. The underlying principle of an immune feedback is based on adaptive control and the designed control estimates fundamental reference grid currents from nonlinear load currents. This control algorithm proposed for DSTATCOM, is validated for maintaining power factor to unity, load balancing and harmonics reduction of supply currents. An improved performance of immune feedback control is presented along with its comparison with conventional control algorithms such as d-q frame, normalized least mean square (NLMS) and other recently developed control algorithms such as leaky LMS, LLMF and synchronous extraction. Experimental results are obtained with the proposed control, which is tested on a prototype developed in the laboratory using a VSC. It is observed from simulation and experimental results that the proposed control algorithm of DSTATCOM is able to achieve mitigation of most of the power quality problems at the distribution level.**

***Keywords*—Power quality; power factor correction; PI controller; immune feedback principle, DSTATCOM**

I. INTRODUCTION

Power engineers are concerned about the rapid increase in power quality (PQ) problems and solutions in the distribution level. Consumers even in developing nations are realizing the importance of good PQ and willing to spend extra cost. Several reasons account for PQ problems in distribution systems viz. an unprecedented increase in power electronics loads, which include converters, switch mode power supplies (SMPS), variable frequency drives, electric arc furnaces, computers etc. Common power quality problems include load unbalancing, voltage regulation, harmonics injection into the grid supply and poor power factor [1]. Guidelines for limiting harmonics and other power quality related problems are specified in IEEE-519 standard [2]. An improvement in quality of power is achieved using different custom power devices and one such recent shunt compensating device is a DSTATCOM (Distribution Static Compensator) [3]. It is used for mitigating power quality problems related to currents, such as reduction of harmonics in grid currents, reactive power compensation, balancing of unbalanced load at distribution level and it can be controlled in different operating modes.

An exhaustive literature review has shown a number of control techniques for the control of shunt compensator [4-19], which are used to estimate the fundamental component of grid reference currents and switching pulses for DSTATCOM. In past few decades, various conventional time domain control methods have been reported for example instantaneous reactive power theory (IRPT) [4], dq frame theory [5], symmetrical components-based modified technique [6], vector resonant controller [7], one-cycle control for three phase shunt compensator with unbalance source and load [8], model predictive control [9]. Several new and promising techniques are also popular viz. unified adaptive linear neuron based control [10], adaptive synchronous extraction [11], normalized least mean square (NLMS) [12-14], recursive least square [15], dual-tree complex wavelet transform [16], predictive current control [17], neural network control [18], and adaptive neuro-fuzzy inference based control [19]. These techniques differ on the basis of complexity, tracking performance, stability and ease of implementation.

Kawafuku et. al. [20] have reported a control algorithm based on biological immune system. The structure of immune feedback system consists of various cells and these have to function in a manner that neutralizes the attack of antigens or foreign invaders. The immune system is a highly evolved system just as the brain. Although neural networks based on working of brain are relatively common. The full potential of biological immune systems is not realized. Its working is based on activities of B-cell, helper and suppressor T-cells and how they work rapidly to respond to foreign particles while quickly stabilizing itself. Its properties of fast control, stabilization, learning and elimination, make it an ideal technique for adaptive control system. These features are helpful in optimization problems, abnormality detection and pattern recognition. However, due to complexity of immune system, such controls have received less attention. Still, some of these controls are successfully used in varied engineering applications [21]. Some of recent applications of immune feedback algorithm include the control of a single phase inverter [22] and a three phase inverter [23], where dead time elimination and space vector PWM control have been used. Simulation studies are reported on the application of immune based feedback principle for a single STATCOM for voltage control [24] as well as multiple STATCOM [25]. However, design, application and experimental implementation of an immune control for solving power quality problems are not reported in the literature.

An immune feedback based control, devised on the working of biological immune system of the human body resembles and works as an adaptive and self-corrective system [26]. In this work, the basic immune technique is utilized for designing a control to mitigate power quality problems. The attack of antigens can be viewed as analogous to the variations in the operating conditions in the system. The control

This article has been accepted for publication in a future issue of this journal, but has not been fully edited. Content may change prior to final publication. Citation information: DOI 10.1109/TIA.2018.2867328, IEEE Transactions on Industry Applications

algorithm is designed to work in two different modes i.e. improvement of power factor for grid currents to unity and regulating AC terminal voltage and to provide load compensation, appropriately. Simulation and test results with the proposed algorithm, demonstrate the unique features of learning, memory and anomaly recognition associated with this algorithm. Performance of proposed control is compared with already reported control algorithms for DSTATCOM such as normalized least mean square (NLMS), dq frame, leaky LMS [27], leaky least mean fourth (LLMF) [28], and adaptive synchronous extraction. The application of this algorithm for shunt compensation is innovative and has not been reported in the literature till date. This also opens a new opportunity to use biologically inspired algorithms on real systems.

II. System Configuration

A block diagram of a three phase DSTATCOM is shown in Fig. 1. A three-phase AC mains with grid impedance, shown using series R_s-L_s branch, feeds a three phase load. The DSTATCOM is designed using a three-phase VSC with a DC bus capacitor at DC side. Passive filters comprising series connected capacitive (C_f) and resistive (R_f) elements at the PCC, are used to suppress switching noise produced by IGBTs (Insulated Gate Bipolar Transistors). This noise contains high frequency components. A nonlinear load is represented in form of a three-phase diode bridge rectifier. A scaled down prototype is implemented in the laboratory and the immune feedback based control is verified under a variety of load changes. Design specifications for simulation and hardware implementation are given in Appendix-A and B.

III. Mathematical Formulation of Control Algorithm

Fig. 2 shows a block diagram of the immune feedback based control algorithm, which is based on the functions of biological immune system of human body and works as an adaptive and self-corrective system. The mathematical expressions related to the immune feedback based control algorithm are given in this section and categorized further in into three sub-sections. The purpose of using the immune feedback principle is to extract the weighted values of the load currents, which correspond to fundamental positive sequence value. The estimation of reference currents is discussed next section followed by the use of PWM (Pulse Width Modulation) current controller for generation of gating pulses.

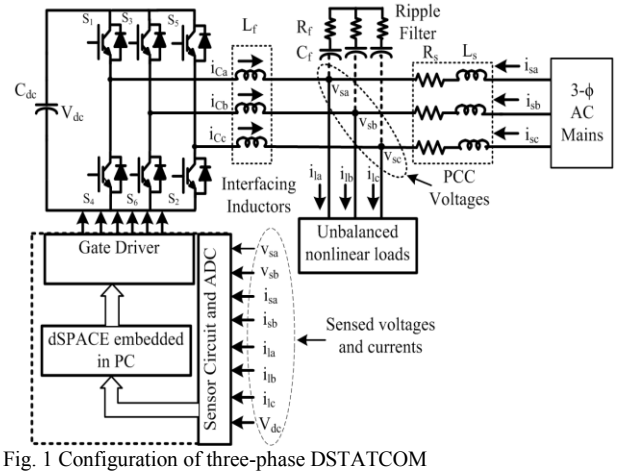

Fig. 1 Configuration of three-phase DSTATCOM

A. Mathematical Approach for Estimation of Weighted Values Using Immune Feedback Algorithm

The peak of PCC (Point of Common Coupling) voltages, is calculated by using 3-phase voltages (v_{sa}, v_{sb}, v_{sc}) as,

$$V_t = \sqrt{2(v_{sa}^2 + v_{sb}^2 + v_{sc}^2)/3} \quad (1)$$

This magnitude (V_t) is used to compute unit inphase and quadrature vectors, which are used to estimate active and reactive components of reference supply currents. In-phase unit vectors of PCC voltages, u_{pa}, u_{pb} and u_{pc} are calculated as follows,

$$u_{pa} = v_{sa}/V_t;\ u_{pb} = v_{sb}/V_t \text{ and } u_{pc} = v_{sc}/V_t \quad (2)$$

These unit inphase vectors are also utilized in the computation of updated active weighted value of reference currents.

The incremental weight based on immune feedback principle at $(n+1)^{th}$ sampling moment is expressed as,

$$\Delta w(n+1) = \eta[1 - \gamma\{\Delta w(n) - \Delta w(n-1)\}^2]\frac{\delta J(n)}{\delta w(n)} + \alpha\Delta w(n) \quad (3)$$

where α is multiplication factor of the foreign materials, parameter η (learning rate) controls the response speed, parameter γ (stabilization factor) controls the stabilization effect and $J(n)$ is the cost function to be minimized and expressed as,

$$J(n) = \frac{1}{2}e(n)^2 \quad (4)$$

Here in (4), $e(n)$ is the error between the sensed value of load current (i_l) and estimated value of current (i_e), is given as,

$$e(n) = i_l - i_e \quad (5)$$

The estimated current is computed using weight vector w^T=[w_p, w_q…] and input vector $x(n)$=[u_p, u_q…], where weight w_p corresponds to the fundamental active component and w_q, is the fundamental reactive weight value extracted from the load current. The parameter u_p, is unit in-phase template and u_q is unit quadrature template of PCC voltages. The estimated load current is product of weight vector (w) and input vector ($x(n)$) given as,

$$i_e = wx^T(n) \quad (6)$$

This weight update rule for immune feedback at $(n+1)^{th}$ sampling moment is stated as,

$$w(n+1) = w(n) + \Delta w(n+1) \quad (7)$$

Rewriting (7) by replacing value of $\Delta w(n+1)$ from (3) and stated at $(n+1)^{th}$ sampling moment as [20],

$$w(n+1) = w(n) + \eta[1 - \gamma\{\Delta w(n) - \Delta w(n-1)\}^2]\frac{\delta J(n)}{\delta w(n)} + \alpha\Delta w(n) \quad (8)$$

The partial differentiation $\frac{\delta J(n)}{\delta w(n)}$ is simplified by the differentiation using chain rule. According to this partial differentiation can be written as, $\frac{\delta J(n)}{\delta w(n)} = \frac{\delta J(n)}{\delta e(n)} \times \frac{\delta e(n)}{\delta w(n)}$.

This article has been accepted for publication in a future issue of this journal, but has not been fully edited. Content may change prior to final publication. Citation information: DOI 10.1109/TIA.2018.2867328, IEEE Transactions on Industry Applications

Differentiation of $\frac{\delta J(n)}{\delta e(n)}$ and $\frac{\delta e(n)}{\delta w(n)}$ give estimated error (*e(n)*) and input vector (*x(n)*) respectively. Therefore, partial differentiation $\frac{\delta J(n)}{\delta w(n)}$ is written in terms of product of estimated error (*e(n)*) and input vector (*x(n)*). Apart from it, weight update equation shows negative learning action if $1>\gamma\{\Delta w(n)-\Delta w(n-1)\}^2>0$ and positive learning action if $1<\gamma\{\Delta w(n)-\Delta w(n-1)\}^2$ and the system is kept stable by choosing appropriate value of learning rate.

The weight updation given in (8), is modified for weighted values corresponding to active power components (w_{lpa}, w_{lpb} and w_{lpc}) of load currents and are given as follows,

$$w_{lpa} = w_{pa} + \eta\left[1-\gamma\{\Delta w_{pa}-\Delta w_{pa}'\}^2\right]e_a u_{pa} + \alpha\Delta w_{pa} \quad (9)$$

$$w_{lpb} = w_{pb} + \eta\left[1-\gamma\{\Delta w_{pb}-\Delta w_{pb}'\}^2\right]e_b u_{pb} + \alpha\Delta w_{pb} \quad (10)$$

$$w_{lpc} = w_{pc} + \eta\left[1-\gamma\{\Delta w_{pc}-\Delta w_{pc}'\}^2\right]e_c u_{pc} + \alpha\Delta w_{pc} \quad (11)$$

The unit quadrature vectors u_{qa}, u_{qb} and u_{qc} are computed from in-phase templates as follows [1],

$$u_{qa} = -u_{pb}/\sqrt{3} + u_{pc}/\sqrt{3} \quad (12)$$

$$u_{qb} = \sqrt{3}\,u_{pa}/2 + (u_{pb}-u_{pc})/2\sqrt{3} \quad (13)$$

$$u_{qc} = -\sqrt{3}\,u_{pa}/2 + (u_{pb}-u_{pc})/2\sqrt{3} \quad (14)$$

These unit quadrature vectors are utilized in computations of reactive weighted values of load currents. The weight update given in (8), is modified for weighted values corresponding to reactive power components (w_{lqa}, w_{lqb} and w_{lqc}) of load currents and are given as,

$$w_{lqa} = w_{qa} + \eta\left[1-\gamma\{\Delta w_{qa}-\Delta w_{qa}'\}^2\right]e_a u_{qa} + \alpha\Delta w_{qa} \quad (15)$$

$$w_{lqb} = w_{qb} + \eta\left[1-\gamma\{\Delta w_{qb}-\Delta w_{qb}'\}^2\right]e_b u_{qb} + \alpha\Delta w_{qb} \quad (16)$$

$$w_{lqc} = w_{qc} + \eta\left[1-\gamma\{\Delta w_{qc}-\Delta w_{qc}'\}^2\right]e_c u_{qc} + \alpha\Delta w_{qc} \quad (17)$$

The average active (w_{lp}) and reactive (w_{lq}) weights are as,

$$w_{lp} = \frac{w_{lpa}+w_{lpb}+w_{lpc}}{3} \quad (18)$$

$$w_{lq} = \frac{w_{lqa}+w_{lqb}+w_{lqc}}{3} \quad (19)$$

The average weight values are used to estimate reference active and reactive weighted values, which is discussed in the next sub section.

B. Estimation of Reference Grid Currents

The DC voltage error (v_{de}) is generated by comparing the sensed voltage at DC bus (V_{dc}) with the reference value (V_{dc}^*). The voltage at DC bus (V_{dc}) is regulated to its reference magnitude by passing error value (v_{de}) to the proportional integral (PI) controller. This control provides an output value which is estimated to be component, w_{pdc}. This component is given at n^{th} sampling instant as,

$$w_{pdc}(n) = w_{pdc}(n-1) + k_{pd}\big(v_{de}(n)-v_{de}(n-1)\big) + k_{id}\big(v_{de}(n)\big) \quad (20)$$

This equation is an expression of PI controller, which is used to regulate voltage at DC bus. Here in (20), parameter w_{pdc} denotes the output of PI controller, k_{pd} is proportional and k_{id} is integral gains. The reference active power weight is calculated by adding w_{lp} and w_{pdc} and is given as,

$$w_p = w_{lp} + w_{pdc} \quad (21)$$

Reference active grid currents (i_{pa}^*, i_{pb}^* and i_{pc}^*) representing three phase components are calculated using inphase unit templates (u_{pa}, u_{pb} and u_{pc}) and reference weight (w_p) as,

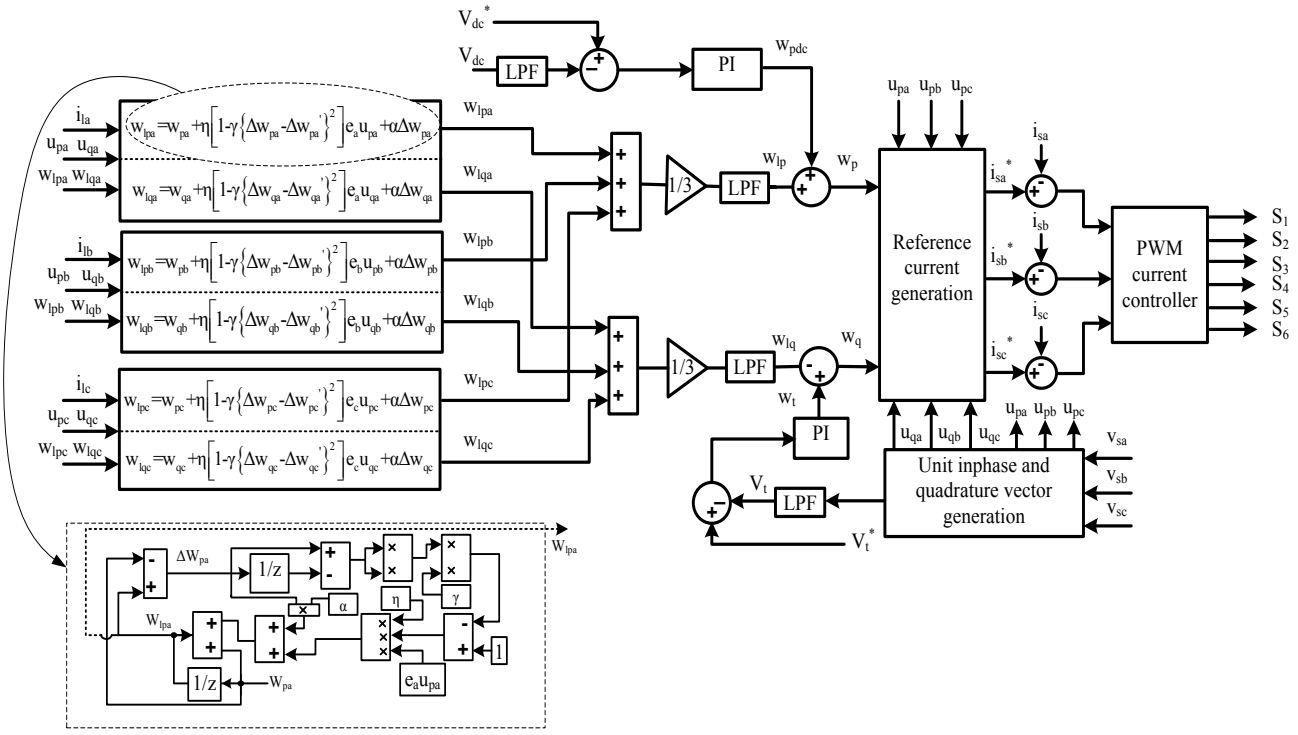

Fig. 2 Block diagram of immune feedback based control algorithm for shunt compensator

This article has been accepted for publication in a future issue of this journal, but has not been fully edited. Content may change prior to final publication. Citation information: DOI 10.1109/TIA.2018.2867328, IEEE Transactions on Industry Applications

$$i_{pa}^{*} = w_p u_{pa}, i_{pb}^{*} = w_p u_{pb} \text{ and } i_{pc}^{*} = w_p u_{pc} \quad (22)$$

These reference active grid currents given in (22) are used to estimate total grid currents.

The PCC voltage magnitude (V_t) is calculated by using (1) and compared with reference PCC voltage (V_t^*), thus the error generated (V_{te}) is passed through a second PI controller to set PCC voltage magnitude at reference value. The output of PCC voltage at n^{th} sampling instant is given as,

$$w_t(n) = w_t(n-1) + k_{pq}\big(V_{te}(n) - V_{te}(n-1)\big) + k_{iq}\big(V_{te}(n)\big) \quad (23)$$

This equation is an expression for a second PI controller used in control algorithm, which is used to regulate voltage at PCC. Here in (23), parameters w_t, k_{pq} and k_{iq} denote PI controller output, its proportional gain and integral gain.

The reference reactive weight (w_q) corresponding to load current, is computed using the average reactive weight (w_{lq}) and the output of second PI controller on AC bus, which gives an estimated output (w_t). This weight w_q, is calculated as follows,

$$w_q = w_t - w_{lq} \quad (24)$$

The reactive reference currents (i_{qa}^*, i_{qb}^* and i_{qc}^*) are computed from the unit quadrature templates (u_{qa}, u_{qb} and u_{qc}), given in (12), (13) and (14), and reference reactive power weight (w_q) as,

$$i_{qa}^{*} = w_q u_{qa}, i_{qb}^{*} = w_q u_{qb} \text{ and } i_{qc}^{*} = w_q u_{qc} \quad (25)$$

Currents computed using (22) and (25) are used to estimate total reference grid currents, which is explained in the next sub section.

C. *Generation of Switching Pulses*

The estimated reference active and reference reactive components of currents given in (22) and (25) are added to estimate reference grid currents. The addition of these current components is given as,

$$i_{sa}^{*} = i_{pa}^{*} + i_{qa}^{*} \quad (26)$$

$$i_{sb}^{*} = i_{pb}^{*} + i_{qb}^{*} \quad (27)$$

$$i_{sc}^{*} = i_{pc}^{*} + i_{qc}^{*} \quad (28)$$

The sensed grid currents (i_{sa}, i_{sb} and i_{sc}) are sensed by the currents sensors and compared with estimated reference currents (i_{sa}^*, i_{sb}^* and i_{sc}^*).Thus, the current errors (i_{sae}, i_{sbe} and i_{sce}) are generated. After the generation of these error signals; these are processed through PWM current controller to produce six switching pulses for six IGBTs switches of VSC.

IV. Simulation Results

The simulation model of the proposed system is developed in MATLAB using the Simulink and Sim Power System (SPS) tool boxes. The behavior of DSTATCOM with the immune feedback principle based control method is verified for power factor correction (PFC) and voltage regulation modes under dynamic load conditions.

A. *Steady State and Dynamic Behavior of DSTATCOM in PFC Mode*

The behavior of a shunt compensator in PFC mode is presented in Figs. 3(a) and (b). These results depict waveforms of PCC voltages (v_s), grid currents (i_s), load currents (i_l), DSTATCOM currents (i_C) and DC bus voltage (V_{dc}). It is noticed from Figs. 3(a) and (b) that the system operates in steady state (before t=0.3s) and the value at DC bus voltage is maintained at reference voltage of 700V by the PI controller.

One phase (phase '*c*') of the load is now turned off (t=0.3s to t=0.4s) and it is noticed that the load currents become unequal and unbalanced. However, the grid currents still remain balanced due to the DSTATCOM action. It is observed from simulated results that under unbalanced load condition, the maximum overshoot, which occurs in DC bus voltage is around 25V. However, it is controlled to 700V (reference value) with a PI controller action within a couple of cycles. The in-phase relationship between the voltages at PCC and the corresponding grid currents is observed and thus power factor correction capability of DSTATCOM is achieved.

The harmonic spectra of grid current (i_{sa}) after compensation and load current (i_{la}) in PFC mode are depicted in Fig. 4. The values of THDs of grid current and load current are observed 2.15%, and 27.10%, respectively. It may be

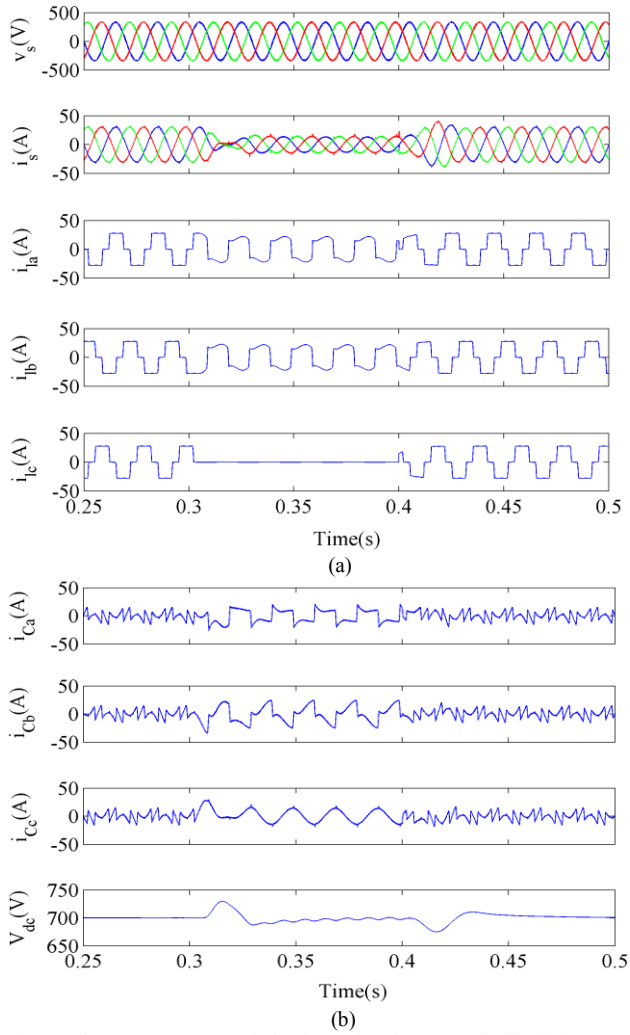

Fig. 3 Shunt compensator behavior using immune feedback in PFC mode

This article has been accepted for publication in a future issue of this journal, but has not been fully edited. Content may change prior to final publication. Citation information: DOI 10.1109/TIA.2018.2867328, IEEE Transactions on Industry Applications

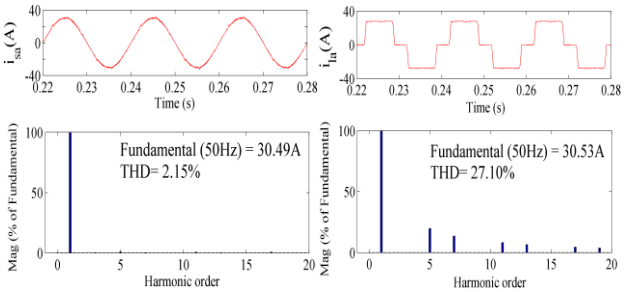

Fig. 4 Harmonic spectra of phase 'a' of (a) grid current, i_{sa} (b) load current, i_{la} in PFC mode

inferred from these results that the harmonic distortion of i_{sa}, is less than a limit (<5%) imposed by international standard such as IEEE-519.

B. *DSTATCOM Performance in Voltage Regulation Mode Under Varying Loads*

The behavior of DSTATCOM is tested at nonlinear load to observe if the voltage is regulated at PCC using proposed control algorithm. The waveforms shown in Figs. 5(a) and (b) represent three-phase voltages at PCC (v_s), 3-phase grid currents (i_s), three-phase load currents (i_l), compensator currents (i_C), self-sustained DC bus voltage (V_{dc}) voltage at the VSC and PCC voltage magnitude (V_t). The system reaches the steady state condition and the voltage at DC bus, V_{dc} of the VSC and PCC voltage magnitude, V_t are regulated at 700V and 338.89 V, which is desired from the control algorithm. The load is changed at t=0.3s, when unbalancing is created in the load and phase 'c' of load is instantly thrown off from the system from t=0.3s till t=0.4s; thereby creating a dynamic load change in the system. However, the grid currents are still observed to be perfectly sinusoidal, having the same peak magnitude and 120° phase displaced from each other due to DSTATCOM operation. The action of the two PI controllers at the PCC voltage and DC bus voltage, regulates both of these voltages to 338.89V and 700V, respectively. Thus, the control algorithm based on an immune feedback adaptively extracts weights under different loading conditions including unbalanced load condition. The voltage regulation is achieved by the action of PI controller within a couple of cycles.

Fig. 6 shows the harmonic spectra of grid current (i_{sa}) after compensation and load current (i_{la}) in voltage regulation mode. Harmonic distortion in phase 'a' of grid current is observed to be 2.97% when the distortion in load current is 27.18%. Fig. 6 clearly highlights that phase 'a' of the grid current, after compensation is maintained sinusoidal and the distortion limits of i_{sa} from harmonics point of view, follow a limit of less than 5% specified by an IEEE-519 standard [2].

C. *Comparative Performance of Immune Feedback Control with NLMS and SRF Control Algorithms*

The critical evaluation of a developed immune feedback control algorithm is made and its performance is compared with NLMS and dq frame control algorithms. The basic mathematical weight update equation for the NLMS control is shown in Appendix-C. Fig. 7 shows a comparative performance of immune feedback and NLMS based control [12-14] developed for control of DSTATCOM.

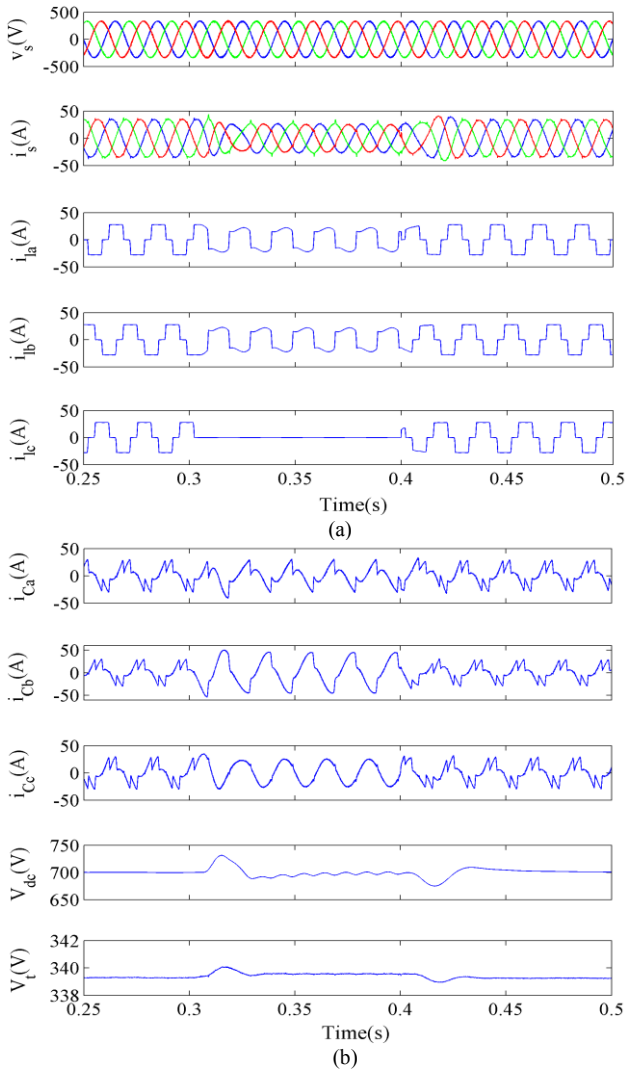

Fig. 5 Shunt compensator behavior with immune feedback based control algorithm in voltage regulation mode

A comparison is also presented in terms of speed of weight convergence, error between sensed and estimated load current, harmonics compensation in grid currents and computational time required for processing both the algorithms. Fig. 7(a) shows convergence of weight corresponding to phase 'a' of load current with immune feedback and NLMS control algorithms. These results present fast weight convergence with immune feedback control algorithm (steady state is obtained at

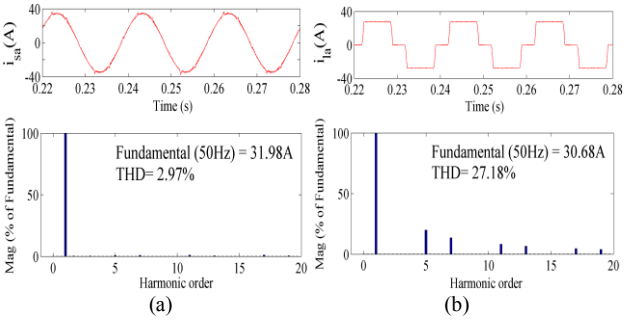

Fig. 6 Harmonic spectra of Phase 'a' of (a) grid current, i_{sa} (b) load current, i_{la} in voltage regulation mode

This article has been accepted for publication in a future issue of this journal, but has not been fully edited. Content may change prior to final publication. Citation information: DOI 10.1109/TIA.2018.2867328, IEEE Transactions on Industry Applications

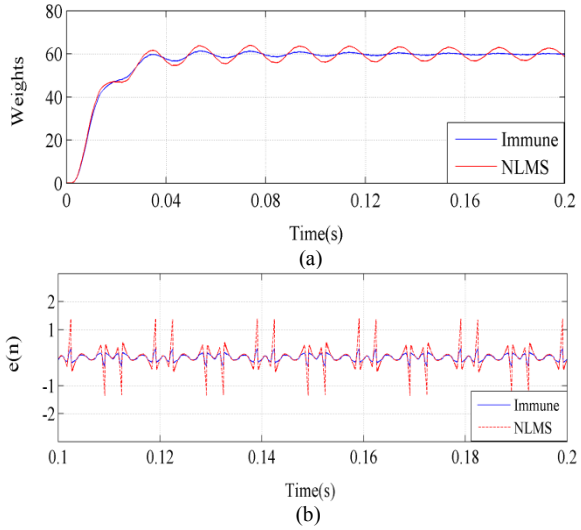

Fig. 7 Comparative performance of immune and NLMS controls in terms of (a) weight convergence (b) error signal

t=0.10s), whereas large sustained oscillations about the average value of weight, are observed with NLMS based control algorithm. Fig. 7(b) shows the error *e(n)* in estimation obtained with both the control algorithms. These results show low error, good tracking speed and fast response with the developed control. Figs. 8(a) and (b) present the harmonic spectrum of grid current (i_{sa}), obtained with NLMS and dq frame control algorithms. These control algorithms are able to achieve 3.33% and 2.75% THDs in grid current, whereas 2.15% THD is achieved with immune feedback based control algorithm (shown in Fig. 4). The control algorithm developed based on immune feedback technique, achieves improved harmonics compensation, fast weight convergence, offers reduced complexity and improved performance in terms of low error and small sampling time required for execution. Another advantage is that this algorithm is PLL-less as compared to dq frame control. The comparative performances of these three control algorithms are summarized in Table-I, which definitely indicates a superiority of proposed control.

D. Comparative Performance of Immune Feedback Control with Leaky LMS, LLMF and SRF Control Algorithms

Performance of immune feedback control is also compared with other adaptive techniques recently proposed in the literature [12-14]. These include leaky LMS, LLMF and synchronous extraction control algorithms. These algorithms viz. leaky LMS and LLMF contain leaky factor and cubic error signal in the weight updation equation, which increases the complexity. A proper selection of leaky factor is a major issue in leaky LMS and LLMF control, because higher value of this factor affects the biased problem and lower value increases Eigen spread [27]. Hence, their complexity is higher due to an immune feedback based control possess less as compared with leaky LMS and leaky LMF (LLMF). Moreover, these results show that the THDs of supply current obtained with leaky LMS and LLMF controls are obtained to be 3.6% and 2.5%, whereas a lower THD value of 2.3% is obtained with an immune feedback control. Another control algorithm reported is based on adaptive theory such as synchronous-extraction based control [11]. This algorithm possesses advantages similar to an immune feedback control. However, THD of supply current obtained with synchronous-extraction based control is 4.4%, which is higher than a THD of supply current obtained (2.3%) with proposed control algorithm. Table-II presents a comparative performance of above control algorithms for DSTATCOM.

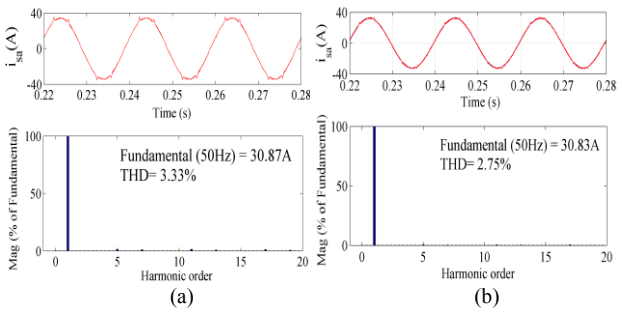

Fig. 8 Harmonic spectra of phase 'a' of grid current, i_{sa} (a) with NLMS and (b) with dq frame controllers in PFC mode

V. Experimental Results

A prototype of the DSTATCOM has been developed in the laboratory for testing the control algorithm. It consists of a three-phase VSC, interfacing inductors, three-phase bridge diode rectifier based three-phase nonlinear load. The control algorithm implementation is performed using DSP (Digital Signal Processor-dSPACE1104) where eight ADC channels are used. The experimental prototype uses Hall Effect voltage (LEM LV-25) and current sensors (LEM LA-25). Test results

TABLE I
COMPARATIVE PERFORMANCE OF IMMUNE FEEDBACK WITH NLMS AND DQ FRAME BASED CONTROL

Features		Immune Feedback	NLMS	dq frame
Modeling		Few mathematical operations are required	Complex require more mathematical operations	Complex-Required Phase lock loop (PLL)
Weight convergence		Fast (steady state at t=0.1s)	Sustained oscillations	NA
Error, *e(n)*		Small	Large	NA
Harmonic compensation	Grid current THD, i_{sa}	30.49A, 2.15%	30.87A, 3.33%	30.83A, 2.75%
	Load current THD, i_{la}	30.53A, 27.10%	30.53A, 27.10%	30.63A, 27.17%
Sampling Time (T_s)		60µs	75µs	60 µs

TABLE II
COMPARATIVE PERFORMANCE OF IMMUNE FEEDBACK WITH LEAKY LMS, LLMF AND SYNCHRONOUS EXTRACTION

Features	Immune Feedback	Leaky LMS	LLMF	Synchronous extraction
Type of Control	Adaptive	Adaptive	Adaptive	Adaptive
Weight convergence	Fast	Slow	Fast	Fast
Static Error	Less	More	Less	Less
Computation	Less	More	More	More
%Harmonics in grid current, i_{sa}	2.3%	3.6%	2.5%	4.4%

This article has been accepted for publication in a future issue of this journal, but has not been fully edited. Content may change prior to final publication. Citation information: DOI 10.1109/TIA.2018.2867328, IEEE Transactions on Industry Applications

have been obtained under a variety of loading conditions and are recorded using standard meters available in the laboratory.

A. Behavior of Immune Feedback Controller for Shunt Compensator

Fig. 9 shows performance of proposed control algorithm in PFC mode at nonlinear load. Fig. 9(a) shows waveforms of phase 'a' of PCC voltage (v_{sa}), its filtered value (v_{saf}), in-phase unit template (u_{pa}) and load current (i_{la}). Fig. 9(b) shows waveforms of sensed DC bus voltage (V_{dc}), filtered DC bus voltage (V_{dcf}), error signal (V_{de}) between reference DC bus and sensed DC bus voltage and output of DC bus PI controller (w_{pdc}). Fig. 9(c) shows waveforms of error signal (e_a), incremental weighted value (Δw_{pa}), delayed weighted value (w_{pa}) and weighted value corresponding to active power component of phase 'a' of load current. Fig. 9(d) shows the average weighted value (w_{lp}) corresponding to active power component of load, output of DC bus PI controller (w_{pdc}) and reference active power weight (w_p) along with w_{lpa}. Fig. 9(e) shows reference supply currents (i_{sa}^*, i_{sb}^* and i_{sc}^*) along with phase 'a' of sensed supply current (i_{sa}). It is observed from these results that the shunt compensator performs satisfactory in steady state and unbalanced load condition using immune feedback control.

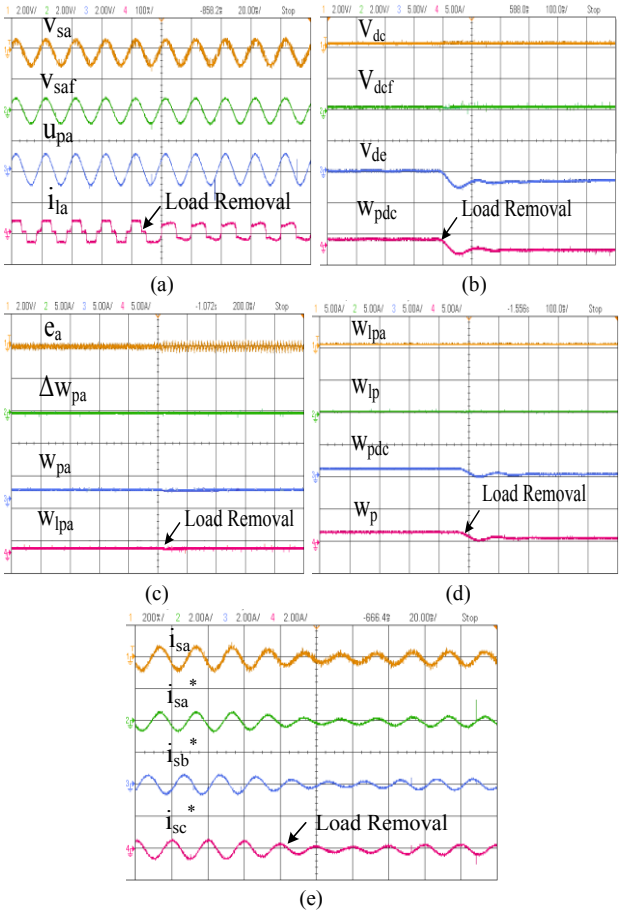

Fig. 9 Experimental performance of shunt compensator with immune feedback based control algorithm (a) v_{sa}, v_{saf}, u_{pa}, i_{la} (b) V_{dc}, V_{dcf}, v_{de}, w_{pdc} (c) e_a, Δw_{pa}, w_{pa}, w_{lpa} (d) w_{lpa}, w_{lp}, w_{pdc}, w_p (e) i_{sa}, i_{sa}^*, i_{sb}^*, i_{sc}^*

B. DSTATCOM Behavior Under Nonlinear Load

Test results are presented in Fig. 10, which show the system behavior when steady state condition has been achieved. Waveforms of PCC voltage and grid current (v_{sa} and i_{sa}), PCC voltage and load current (v_{sa} and i_{la}) and PCC voltage and compensator current (v_{sa} and i_{Ca}) are shown in Figs. 10(a)-(c). Harmonic spectra corresponding to phase '*a*' of grid current (i_{sa}), load current (i_{la}) and PCC voltage are shown in Figs. 10(d)-(f). The observed percentage of THDs in grid current, load current and PCC voltage are 2.3%, 22.9% and 3.2% respectively. It can be observed from the system responses that the DSTATCOM performs the function of correcting the power factor of grid current when nonlinear load is connected. The THD results show a reduction from 22.9% to 2.3% achieving harmonics reduction to a very large extent.

C. Dynamic Behavior Under Varying Nonlinear Load

Figs. 11(a)-(d) show the test results obtained with the shunt compensator when a nonlinear load is also varying. Fig. 11(a) shows the PCC voltage (v_{sa}) and the three phase grid currents (i_{sa}, i_{sb} and i_{sc}) when unbalanced condition is introduced suddenly. These results point out that the grid currents have decreased in magnitude, however, are sinusoidal and balanced. Fig. 11(b) shows the PCC voltage (v_{sa}) of phase 'a', and phase 'a', 'b' and 'c' currents drawn by the load (i_{la}, i_{lb} and i_{lc}) when the load in phase 'c' is suddenly disconnected. Fig. 11(c) shows the PCC voltage (v_{sa}) and the three phase compensator currents (i_{Ca}, i_{Cb} and i_{Cc}) under the same load dynamics. Moreover, it is simultaneously seen from these

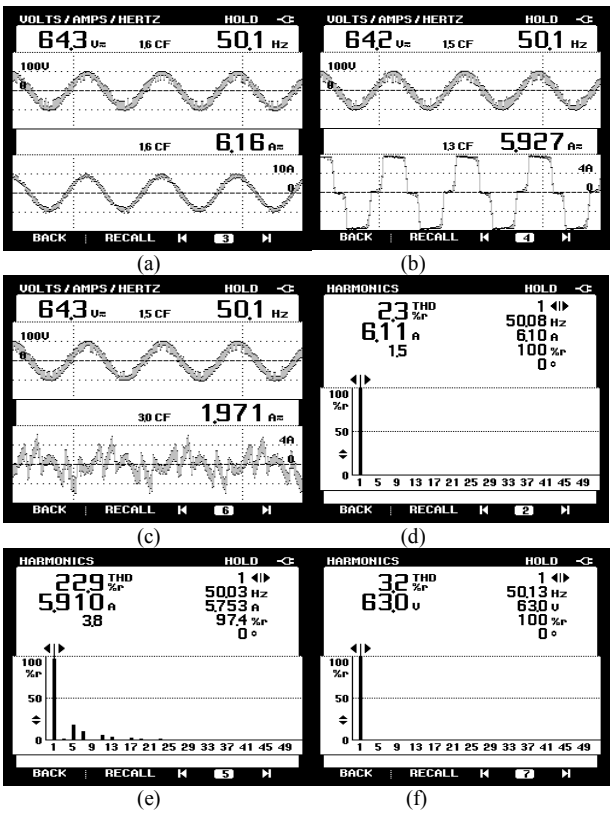

Fig. 10 Steady state behavior for power factor correction using DSTATCOM with nonlinear load (a)-(c) waveforms of grid current, i_{sa} load current, i_{la} and compensator current, i_{Ca} along with v_{sa} (d)-(f) harmonic spectra of i_{sa}, i_{la} and v_{sa}

This article has been accepted for publication in a future issue of this journal, but has not been fully edited. Content may change prior to final publication. Citation information: DOI 10.1109/TIA.2018.2867328, IEEE Transactions on Industry Applications

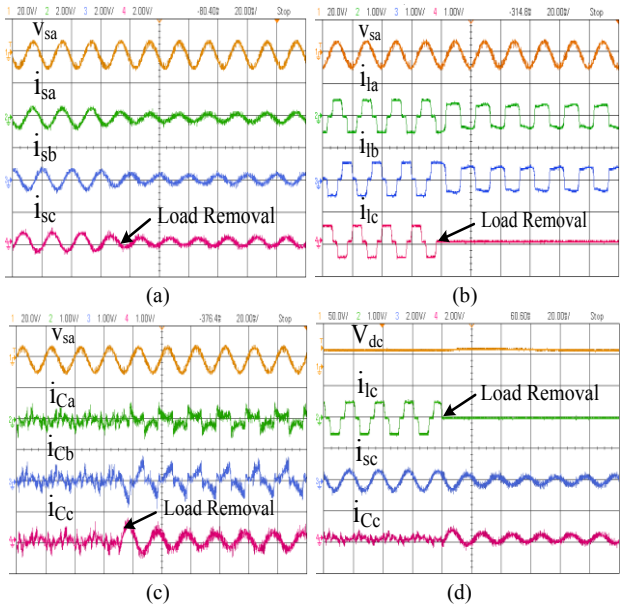

Fig. 11 Experimental results of the system under dynamic load conditions (a) v_{sa}, and grid currents (i_{sa}, i_{sb}, i_{sc}) (b) v_{sa}, and load currents (i_{la}, i_{lb}, i_{lc}) (c) v_{sa}, and compensator currents (i_{Ca}, i_{Cb}, i_{Cc}) (d) V_{dc}, i_{lc}, i_{sc}, i_{Cc}

results that the compensator now injects higher currents. Fig. 11(d) shows the waveforms of DC bus voltage (V_{dc}), load current (i_{lc}) grid current (i_{sc}) and compensator current (i_{Cc}) of phase 'c'. These results confirm that closed loop immune feedback control algorithm is stable and regulates the DC bus voltage at its 200V (set value) within couple of cycles during unbalanced load currents.

VI. Conclusions

A control algorithm based on immune feedback principle has been developed for the control of DSTATCOM. It has been designed and implemented for improving several power quality problems at distribution level. Extensive test results backed with simulation results have been presented for proposed control algorithm. The control algorithm has been developed and implemented for generating switching pulses for VSC. Superior performance of an immune feedback control algorithm has been observed in terms of convergence speed, harmonics compensation, error minimization and computational complexity then it has been compared with NLMS and dq frame based control algorithms for DSTATCOM. Further comparisons with other adaptive controls viz. leaky LMS, LLMF and synchronous extraction are tabulated in Table -II. These results show that the proposed immune control algorithm works well at closed loop conditions and also responds well under extreme load variations. Test results validating the simulation results have recorded 2.3% THD in the grid current obtained after compensation, thereby meeting the standard IEEE-519 limits for harmonics. The obtained value of THD of supply currents is among the lowest of all the considered algorithms. This work highlights the following outcomes.

- Biological immune feedback control algorithm has suitably been designed and implemented to improve power quality problems.
- The immune control algorithm has been found to have an inherent capability to adapt, recognize patterns, identify, self organize and learn. The proposed control algorithm mimics this behavior quite well.
- Experimental results highlight the feasibility of depicting a complex biological phenomenon in a simplified manner.
- A good match between experimental results and simulated results points to feasibility of such control algorithm.
- The performance of developed control has been compared to a number of conventional as well as recently proposed control algorithms and it gives improved performance. Although all the control algorithms have been successful in reducing harmonics substantially (<5%) in the supply current, however, the best performance has been achieved with the proposed control algorithms under similar test conditions.
- The concept and working of biological algorithms can be used a tool to design controllers for real time systems.

This work highlights in detail the design, working and application of the proposed control algorithm in solving power quality problems and used for load compensation.

Appendix-A

AC Supply: 415V, 3-ph and 50Hz; grid impedance: R_s=0.01Ω, L_s=1mH; reference DC bus voltage V_{dc}=700V; DC bus capacitor C_{dc}=1640μF; interfacing inductor L_f=3mH; ripple Filter R_f=5Ω, C_f=5μF, DC bus PI proportional and integral gains: k_{pd}=0.5, k_{id}=0.02; learning rate factor (η)=0.045, stabilization factor (γ)=0.32, load: diode rectifier with R=15Ω, L=100mH.

Appendix-B

AC Supply: 110V, 3-ph and 50Hz; grid impedance: R_s=0.3Ω, L_s=1mH; reference DC bus voltage V_{dc}=200V; DC bus capacitor C_{dc}=1640μF; interfacing inductor L_f=3mH; DC bus PI proportional and integral gains: k_{pd}=0.3, k_{id}=0.05; load: diode rectifier with R=15Ω, L=100mH.

Appendix-C

Mathematical formulation for NLMS controller as [12-14],

A *posteriori* estimation error at the n^{th} instant is given as,

$$\acute{\varepsilon}(n) = \varepsilon(n)\left[1 - \mu(n)x^T(n)x(n)\right] \quad (29)$$

If step size $\mu(n) = \frac{1}{x^T(n)x(n)}$, then $\acute{\varepsilon}(n)$ becomes zero. Under this condition, the recursive weight equation is formulated as,

$$w(n+1) = w(n) + \frac{e(n)x(n)}{x^T(n)x(n)} \quad (30)$$

Another variation of this NLMS algorithm is shown in (31) where α' is the new normalized adaptation constant and λ is a small positive number.

$$w(n+1) = w(n) + \frac{\alpha' e(n)x(n)}{\lambda + x^T(n)x(n)} \quad (31)$$

The need of λ arises to ensure the weight updation does not become excessively large even if $x^T(n)x(n)$ becomes small temporarily.

Acknowledgement

The authors would like to thank Department of Science and Technology, Government of India, for the sponsored project (grant EMR/2016/001874).

AUTHOR INFORMATION

Manoj Badoni (manojbadoni23@gmail.com) is with the Department of Electrical and Instrumentation Engineering Thapar University, Patiala, India. **Alka Singh** is with the Department of Electrical Engineering, Delhi Technological University, Delhi, India. **Bhim Singh** is with the Department of Electrical Engineering, Indian Institute of Technology, Delhi, India. **Alka Singh** is Senior Member of the IEEE and **Bhim Singh** is Fellow of the IEEE. This article first appeared as "DSP based implementation of an immune feedback algorithm for control of shunt compensator" at the 2016 IEEE 6th International Conference on Power Systems (ICPS). This article was reviewed by the IEEE-IAS Industrial Automation and Control Committee.

REFERENCES

[1] B. Singh, A. Chandra, K. Al-Haddad, *Power Quality: Problems and Mitigation Techniques*, John Wiley and Sons, U.K., 2015.

[2] *IEEE Recommended Practices and Requirement for Harmonic Control on Electric Power System*, IEEE Std.519, 1992.

[3] S. R. Arya, B. Singh, R. Niwas, A. Chandra and K. Al-Haddad, "Power quality enhancement using DSTATCOM in distributed power generation system," *IEEE Trans. Indu. Applications*, vol. 52, no. 6, pp. 5203-5212, Nov.-Dec. 2016.

[4] H. Akagi, Y. Kanazawa and A. Nabae, "Generalized theory of the instantaneous reactive power in three-phase circuits," in *Proc. IEEE and JIEE IPEC*, pp. 821–827, 1983.

[5] M. B. Latran, A. Teke and Y. Yoldaş, "Mitigation of power quality problems using distribution static synchronous compensator: a comprehensive review," *IET Power Electronics*, vol. 8, no. 7, pp. 1312-1328, 2015.

[6] R. Kumar, B. Singh and D. T. Shahani, "Symmetrical components-based modified technique for power-quality disturbances detection and classification," *IEEE Trans. Ind. Applications*, vol. 52, no. 4, pp. 3443-3450, July-Aug. 2016.

[7] H. Yi, F. Zhuo,Y. Zhang, Y. Li, W. Zhan, W. Chen and J. Liu, "A source-current-detected shunt active power filter control scheme based on vector resonant controller," *IEEE Trans. Indu. Applications*, vol. 50, no. 3, pp. 1953-1965, May-June 2014.

[8] J. Taotao and K. M. Smedley, "Operation of one-cycle controlled three phase active power filter with unbalanced source and load," *IEEE Trans. Power Electron.*, vol. 21, pp. 1403-1412, 2006.

[9] L. Tarisciotti, A. Formentini, A. Gaeta, M. Degano, P. Zanchetta, R. Rabbeni and M. Pucci, "Model predictive control for shunt active filters with fixed switching frequency," *IEEE Trans. Indu. Applications*, vol. 53, no. 1, pp. 296-304, Jan.-Feb. 2017.

[10] M. Qasim, P. Kanjiya and V. Khadkikar, "Optimal current harmonic extractor based on unified ADALINEs for shunt active power filters," *IEEE Trans. Power Electron.*, vol. 29, pp. 6383–6393, 2014.

[11] B. Singh, S. R. Arya, A. Chandra and K. Al-Haddad, "Implementation of adaptive filter in distribution static compensator," *IEEE Trans. Indu. Applications*, vol. 50, no. 5, pp. 3026-3036, Sept.-Oct. 2014.

[12] A. Singh, M. Badoni and B. Singh, "Application of least means square algorithm to shunt compensator: An experimental investigation," in *Proc. IEEE Inter. Conf. on Power Electronics, Drives and Energy Systems (PEDES)*, Mumbai, pp. 1-6, 2014.

[13] S. Haykin, *Adaptive Filter Theory*, Pearson Publications, 2002.

[14] R. K. Agarwal, I. Hussain and B. Singh, "Grid integration of single stage SPV system using NLMS filtering control technique," in *Proc. IEEE 6th International Conf. on Power Systems (ICPS)*, New Delhi, pp. 1-6, 2016.

[15] M. Badoni, A. Singh and B. Singh, "Variable forgetting factor recursive least square control algorithm for DSTATCOM," *IEEE Trans. Power Del.*, vol. 30, no. 5, pp. 2353-2361, 2015.

[16] R. Kumar, B. Singh, D. T. Shahani and C. Jain, "Dual-tree complex wavelet transform-based control algorithm for power quality improvement in a distribution system," *IEEE Trans. Ind. Electron.*, vol. 64, no. 1, pp. 764-772, Jan. 2017.

[17] K. Venkatraman, M. P. Selvan and S. Moorthi, "Predictive current control of distribution static compensator for load compensation in distribution system," *IET Gen., Trans. & Distri.*, vol. 10, no. 10, pp. 2410-2423, 2016.

[18] B. Singh, P. Jayaprakash, S. Kumar and D. P. Kothari, "Implementation of neural-network-controlled three-leg VSC and a transformer as three-phase four-wire DSTATCOM," *IEEE Trans. Indu. Applications*, vol. 47, no. 4, pp. 1892-1901, July-Aug. 2011.

[19] M. Badoni, A. Singh and B. Singh, "Design and Implementation of ANFIS Based Control Algorithm for DSTATCOM," *Electric Power Components & Systems*, vol. 43, no. 15, pp. 1741-1751, 2015.

[20] M. Kawafuku, M. Sasaki and K. Takahashi, "Adaptive learning method of neural network controller using an immune feedback law," in *Proc. IEEE/ASME Inter.Conf. on Advanced Int. Mech.*, pp. 641 – 646, 1999.

[21] Dipankar Dasgupta, "Advances in artificial immune systems," *IEEE Com. Intelligence Magazine*, vol. 1, iss. 4, pp. 40-49, Nov. 2006.

[22] J. Yuan, Z. Zhao, Cong Li, Jin Wang and C. Tian, "An immune algorithm based dead time elimination PWM control strategy in a single phase inverter," in *Proc. IEEE APEC*, pp. 757-764, 2013.

[23] J. Yuan, J. Pan, W. Fei, C. Cai and B. Chen, "An immune algorithm based space vector PWM control Strategy in a three phase inverter," *IEEE Trans. Ind. Electron.*, vol. 60, no. 5, pp. 2083-2094, May 2013.

[24] H. F. Wang, H. Li and H. Chen, "Application of cell immune response modeling to power system voltage control by STATCOM," *IEE Proc.-Generation, Trans. and Dist.*, vol. 149, pp. 102-107, May 2002.

[25] H. F. Wang, H. Li and H. Chen, "Power system voltage control by multiple STATCOMs based on learning humoral immune response," *IEE Proc.- Gen., Trans. & Dist.*, vol. 149, no. 4, pp. 416-426, July 2002.

[26] M. Badoni, A. Singh and B. Singh, "DSP based implementation of an immune feedback algorithm for control of shunt compensator," in *Proc. IEEE 6th Inter.Conf. on Power Systems (ICPS)*, New Delhi, pp. 1-6, 2016.

[27] S. R. Arya and B. Singh, "Performance of DSTATCOM using leaky LMS control algorithm," *IEEE Journal of Emerging and Selected Topics in Power Electronics*, vol. 1, no. 2, pp. 104-113, June 2013.

[28] R. K. Agarwal; I. Hussain; B. Singh, "Implementation of LLMF control algorithm for three-phase grid tied SPV-DSTATCOM system," *IEEE Transactions in Early Access*.